

RESEARCH ARTICLE

Optimized manufacturing and temperature-dependent structural and property analysis of multi-phase functionally graded materials

K. Sainath^{1*}, R. Karuppasamy¹, S. Prabakaran²

¹Department of Mechanical Engineering, Faculty of Engineering, Karpagam Academy of Higher Education, Coimbatore-641 021, Tamil Nadu, India

²Karpagam Innovation and Incubation Council, Coimbatore-641 021, Tamil Nadu, India

Phone: +9842523681; Fax.: +0422-2980022

ABSTRACT - The functionally graded materials (FGMs) have been realised to be potential candidates when it comes to high-pressure projects and applications where thermal and mechanical stability are to be ensured in extreme environments. In the research, the drawback of the widely used stainless steel SS316L, which faces high-stress conditions in thermal environments, will be overcome by the innovation of two new FGMs composed of SS316L and Inconel 625, Ti6Al4V, and Inconel 718. The aim was to conduct the fabrication and testing of a multi-phase FGM with the help of advanced techniques of manufacturing, namely additive manufacturing and powder metallurgy, with the strict control of layer thickness of 0.2 mm and contents of its materials (60% SS316L, 20% Inconel 625 or Ti6Al4V, and 20% Inconel 718). Tensile testing, yield testing, fatigue, and creep behaviour were performed at temperatures of -20°C and $+60^{\circ}\text{C}$. The findings indicated that the FGM containing SS316L, Inconel 625, and Inconel 718 proved to be superior to SS316L at every point, where its tensile strength is 992 MPa and its yield strength is 602 MPa, also at a temperature of $+60^{\circ}\text{C}$ versus 460 MPa and 186 MPa tensile and yield strengths in SS316L. The advanced fatigue performance and creep resistance were also indicated due to the better qualities of the Inconel alloys. Such results are indicative of the gradient composition and layer formation that augment thermal and mechanical capabilities. The research concludes that these FGMs can be considered excellent prospects for the aerospace and power generation industries, where strength and thermal endurance are essential for the next generation of the industry.

ARTICLE HISTORY

Received : 05th Feb. 2025
 Revised : 17th July 2025
 Accepted : 08th Sept. 2025
 Published : 30th Sept. 2025

KEYWORDS

Advanced Manufacturing
Optimization
Mechanical properties
Functionally graded materials
Thermal stability
Mechanical properties

1. INTRODUCTION

A maritime grading of composite materials with non-homogeneous spatial property distributions has emerged in recent times [1]. Through the grading of a material's internal constitution, its properties are intentionally controlled during the production process. They are created as either stepwise-graded or continuous-graded materials, depending on the production method [2]. Laminates are classic examples of stepwise-graded composites, which suffer from the disadvantage of discontinuity of stress on the interfaces between neighboring discrete layers [3]. Functionally graded materials (FGMs) are materials whose properties are continuously varying, and they suffer from none of this disadvantage. Today, FGMs often comprise two disparate materials with increasingly varying percentages of volume of the constituents, which provides them with characteristics that are easy to use and undergo alterations in a particular manner [4]. To produce graded lightweight films and bulk FGMs, several manufacturing processes are available. The four methods of processing categories are the following: in-situ analysing strategies (laser cladding, spray forming, sedimentation, crystallization, centrifugal casting, etc.); powdered strategies (dry powdered analysing, slip vesting, tape moulding, penetration process or electrochemical progress, powdered injection moulding, and self-generate high-temperature synthesis); rapid prototyping strategies (multiphase jet crystallization, 3D-printing, laser printing, laser sintering), in-situ processing methods (laser siding, spray building up, sedimentation, and crystallization, centrifugal casting), and deposition processes (chemical vapor deposition, physical vapour deposition, electrophoretic deposition, slurry depositing, pulsed laser deposition, plasma spraying) [5].

Due to the widespread usage of FGM in sandwich constructions and functionally graded materials, several researchers have examined the performance and strength of these materials in recent years. A researcher must have a thorough understanding of FGM structures before exploring FGM sandwich structures. [6] proposed an approach to investigate the shape and vibration control of plates composed of functionally graded materials with integrated piezoelectric sensors and actuators using finite element analysis based on conventional laminated plate theory. Yang and other researchers studied how FGM plates vibrate and make sounds in hot conditions [7]. They discovered that the way the materials are spread out and the temperature significantly affect how these plates vibrate and produce noise. Wang and others. A study examined the behavior of vibrating plates composed of special materials that undergo a gradual change when they move in a straight line. To explore this behavior, the researchers applied the Galerkin technique and the d'Alembert principle. Research by [8] investigated the free vibration of functionally graded plates. To study how changes in material properties

*CORRESPONDING AUTHOR | K. Sainath | ✉ sainath0318@gmail.com

change vibration, they used random geometric analysis. Since the properties of the material were not always predictable, and because stiffness and weight are closely related, this had a substantial impact on the way the plates behaved. When examining vibration and flutter in supersonic porous FGM plates, the work by [8] provides a common approach to handling both regular and irregular boundary conditions. Using a special type of plate with different properties in two directions and some shape flaws, we examined how this plate vibrated when subjected to a regular force. [9] discovered how this combined to affect how the plate's vibrations behaved at resonance by altering how the materials were set in layers and with these shape flaws. A 3D theory of how materials bend and vibrate was combined with a computer technique to explore how flexible plates of two different material types bend or vibrate freely. Double-layer FGM plates with metal connections, stacked on elastic foundations, were evaluated by Nguyen, who used Navier's solution approach in conjunction with the finite element method to determine their mechanical characteristics [9].

Functionally graded materials are specialized materials that can withstand extremely high temperatures while maintaining their strength. Their properties change smoothly from one side to another by gradually mixing their different parts [10]. Due to these unique features, FGMs are receiving considerable attention in various industries, particularly in high-temperature environments such as those found in space shuttles, airplanes, and nuclear reactors. Many research papers have been written on this topic over the years. When FGMs are used to protect against heat and are held in place, they can experience large strains and stresses when temperatures are high [11]. This creates a certain level of tension that can lead to bending or other shape changes. It is expected that changes in material properties with temperature can make the materials' response to stress more complex. This means we need to study how FGMs behave when they buckle carefully and after they buckle, considering that their properties change with temperature.

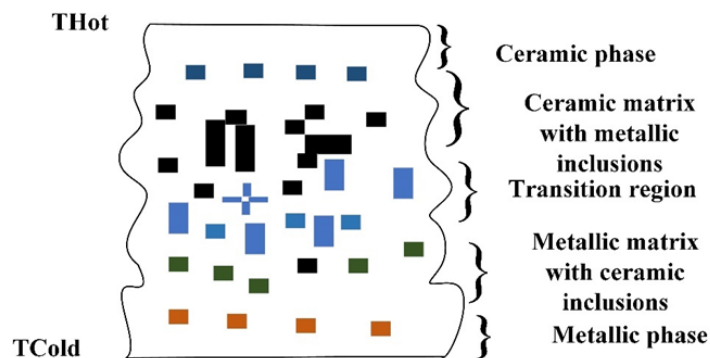


Figure 1. Structural view of continuously graded FGM

Special materials known as FGM can withstand extremely high temperatures and retain their strength. By grading their parts, their properties change smoothly, one transitioning into another. As a result, these FGMs receive considerable attention due to their unique features in various industries with high-temperature applications, such as space shuttles, airplanes, and nuclear reactors. This topic has been explored in numerous research papers over the years [12]. Large strains and stresses may occur in FGMs when they are used to protect structures against heat and are subjected to external loads. This creates a certain level of tension that can lead to bending or other shape changes. It is expected that changes in material properties with temperature can make the materials' response to stress more complex. This means we need to study how FGMs behave when they buckle carefully and after they buckle, considering that their properties change with temperature [13].

In this study, two new FGM materials are introduced by integrating SS316L with other high-performance alloys: The first FGM designed in this research work is SS316L + 20% Inconel 625 + 20% Ti6Al4V, in which SS316L is blended with two high-performance metals. Inconel 625 is a nickel-based superalloy that exhibits high resistance to oxidation and corrosion, particularly when exposed to high temperatures. It exhibits excellent characteristics of fatigue and creep resistance, making it applicable in high-temperature conditions [14]. Ti6Al4V, also known as titanium grade 5, is distinguished by its exceptional mechanical properties at both high and low temperatures, a remarkable strength-to-weight ratio, and notable resistance to corrosion. The enhanced mechanical properties of SS316L envisaged in this FGM include tensile strength, fatigue strength, and thermal stability. Inconel 625 and Titanium Grade 5 enhance the activities of the SS316L matrix in the fabrication of this FGM [15]. It is believed that the combination will enhance the material's performance under demanding conditions, such as high mechanical loads and thermal stresses, making it suitable for the aerospace, chemical, and power generation industries. The second composite material under discussion is composed of SS316L, 20% Inconel 625, and 20% Inconel 718, which are two high-temperature nickel-based superalloys reinforced by SS316L. Inconel 718 is similar to Inconel 625 as far as high-temperature oxidation is concerned, but possesses higher creep strength, tensile and fatigue strength, and structural stability at temperatures much above 700 °C [16]. This makes Inconel 718 ideal for long-term high-temperature applications where materials are subjected to mechanical and thermal loading stresses. The incorporation of both Inconel 625 and Inconel 718 into the SS316L matrix aims at achieving an FGM with improved mechanical properties, thermal stability, and resistance to creep and fatigue at high operating temperatures, in addition to the inherent corrosion resistance offered by SS316L [17]. This combination is particularly

effective for critical, high-reliability applications, including turbine blades, heat exchangers, and other components of equipment that operate under harsh conditions for an extended period [18].

By incorporating these progressive alloys into SS316L, it is presumed that both FGMs will outperform the base metallic SS316L in terms of mechanical and thermal limitations associated with extreme functional states in both low- and high-temperature applications. These new FGMs are expected to enhance properties such as mechanical strength, toughness, and improved performance in terms of creep compared to the base material SS316L. There are expected improvements in the aforementioned materials, including increased resistance to thermal expansion, oxidation, and fatigue, making them suitable for more aggressive applications than SS316L. In this work, an attempt will be made to assess the new materials quantitatively for their high-temperature capabilities under extreme conditions, such as stressed environments, in order to gather extensive data on the materials' suitability for high-stress and high-temperature use. The creation of FGMs is necessary due to the limitations of SS316L in high-temperature environments, including decreased mechanical strength and creep resistance. To overcome these obstacles and enhance thermal stability, tensile strength, and yield strength in demanding industrial applications, this study investigates the potential of FGMs, which incorporate cutting-edge alloys such as Inconel 625, Inconel 718, and Ti6Al4V.

2. MATERIALS AND METHODS

2.1 Materials Preparation

The fabrication of FGM samples in this study was carried out using a combined approach of Additive Manufacturing (AM) and Powder Metallurgy (PM) to precisely engineer gradient structures that deliver superior mechanical and thermal performance. The two FGMs developed, FGM-1 (60% SS316L + 20% Inconel 625 + 20% Ti6Al4V) and FGM-2 (60% SS316L + 20% Inconel 625 + 20% Inconel 718), were chosen based on their synergistic properties, which are suitable for extreme temperature applications. The process began with the Preparation of raw materials: high-purity metal powders ($\geq 99.9\%$) of SS316L, Inconel 625, Inconel 718, and Ti6Al4V were selected with particle sizes ranging between 10 μm and 45 μm [19]. These powders were dried in a vacuum oven to eliminate moisture and then stored in inert conditions. The powders for each composite formulation were then homogenized through high-energy ball milling at 200 rpm for four hours in an argon atmosphere to prevent oxidation and ensure uniform particle distribution. The FGMs were constructed by designing a multilayer structure in which five different compositional layers, each having a width of 0.2 mm, were stacked up to form a gradient from pure SS316L at the bottom to the target alloy blend at the top [20]. The thermal stability, stress distribution, and deformation behavior of this design were modeled using CAD software (SolidWorks) and finite element simulation in ANSYS Workbench prior to physical manufacturing. Gradients were printed through additive manufacturing using a Directed Energy Deposition (DED) system, during which a fundamental capability of the DED process—precise control over the delivery of feedstock and laser power—was leveraged to print each gradient layer accurately [21]. In the powder metallurgy route, the powders were manually filled layer by layer in a graphite die, then compacted at 750 MPa. This was followed by sintering in a vacuum furnace at 1200°C for two hours to consolidate the structure. All samples were heat-treated in a stress-relief process at 600°C for 1 hour after fabrication to reduce residual stresses. We machined the fabricated FGMs into standardized test specimens using wire Electrical Discharge Machining (EDM) based on ASTM standards. During this thesis, the microstructural integrity and integration bonding between layers were assessed using optical microscopy and SEM, while the elemental distribution across the gradient was verified via Energy Dispersive X-ray (EDX) Spectroscopy. The FGM design was documented using CAD renderings, along with cross-sectional images of actual samples, to clarify the gradient architecture. Through this comprehensive methodology, robust FGM samples were fabricated to meet and exceed the challenges posed by thermal and mechanical environments for which they are intended.

2.2 Mechanical Property Testing in Functionally Graded Materials

Mechanical property evaluation is crucial for assessing the suitability of a material for applications that are subject to high stress, large cycles of loading, and extreme temperatures. In this study, four primary mechanical properties that are necessary for comparing the developed FGMs with conventional SS316L stainless steel are presented: Ultimate Tensile Strength (UTS), yield strength (0.2% proof stress), fatigue resistance, and creep behavior. The uniaxial tensile test was used to determine the tensile and yield strengths at two different temperatures: -20°C (to simulate a low-temperature industrial environment) and $+60^\circ\text{C}$ (representing elevated temperature operating conditions in the aerospace and power generation sectors) [22]. The trend observed across all materials was that mechanical strength decreased with increasing temperature; however, FGMs demonstrated significant superiority over SS316L under both conditions. Tensile testing was conducted on an Instron 5969 tensile testing machine with a strain rate of 10^{-3} s^{-1} . Specimens were prepared using additive manufacturing with dimensions following ASTM E8 standards. Tests were performed in a temperature-controlled chamber at -20°C and $+60^\circ\text{C}$, and each condition was repeated three times to ensure data consistency [23].

2.3 Structural Analysis

2.3.1 Low-temperature analysis

To assess the performance of newly developed functionally graded materials (FGMs) under sub-regional conditions, a series of mechanical tests was conducted at low temperatures ranging from -50°C to -100°C . The tensile test was done using cooled, standardised samples in a controlled thermal chamber to simulate the rigid industrial environment. The test

setup involves applying a uniaxial tensile load until failure, enabling the evaluation of mechanical strength, including the final tensile strength, yield stress, and the increase under low-temperature stress. The hardness was tested using the Wickers and Brinell methods, where indents were made on the surface after conditioning it at sub-zero temperatures. These test deformations were important to assess surface resistance, especially for effects or wearers in cryogenic conditions. Additionally, control effects were conducted on the tested samples, which were balanced for the target cold temperature. These tests helped determine the material's resistance to brittle fractures by measuring the energy absorbed during the sudden impact. The combination of these tests provided a comprehensive understanding of FGM's flexibility, strength, and impact resistance at low temperatures, which is necessary to evaluate its reliability in extreme cold applications, such as aerospace, cryogenic systems, and offshore structures [24].

2.3.2 High-temperature analysis

To evaluate the high-temperature performance of the developed functionally graded material (FGM), a comprehensive set of mechanical tests was conducted at high temperatures ranging from 300 °C to 1000 °C, under aerospace, power generation, and real-world conditions in a high-temperature environment. A high-temperature tensile testing machine, equipped with a thermal chamber, was used to conduct tensile testing. The samples were gradually heated to the target temperature, equilibrated for thermal balance, and then subjected to unique loading until failure. It allowed measuring the strength of the yield, tensile strength, and increase at various temperatures, helping to identify the range in which FGM maintains structural integrity. Hardness testing was done on pre-pruning samples at each specified temperature using high-temperature-compatible indenters. These tests helped assess the surface resistance of FGMS for deformation under thermal stress and wear conditions. Additionally, creep testing was conducted by applying continuous loads to samples at 600 °C and 1000 °C for extended periods of time. Over time, deformation of materials was recorded to evaluate their long-term dimensional stability under constant stress. This data provided significant insight into the GM suitability FGM y for components under turbine blades and heat exchanges, such as those with a longer temperature service [25].

2.3.3 Fatigue and creep analysis

To comprehensively evaluate the mechanical durability of the developed functionally graded material (FGM), fatigue and creep tests were conducted under controlled laboratory conditions and at high temperatures. Fatigue testing included individual stress dimensions and samples for cyclical loading at temperatures that simulate real-world operating conditions, such as those encountered in engines or rotating devices. The trials were performed using an allot-hydrolyric fatigue test machine, where the samples were repeatedly loaded and unloaded until failure [26]. This enables the generation of the S-N curve, which illustrates the relationship between failure and the number of cycles for the applied tension levels. These tests helped determine the fatigue life of FGMS and assess their resistance to initiation and spread over time. In addition, creep tests were conducted by applying a continuous load to samples maintained at high temperatures of 600 °C and 1000 °C using high-temperature creep test mechanisms. Under thermal stress, deformation was constantly monitored over an extended period to measure the resistance of materials to time-dependent stress. Additionally, creep tests were conducted to determine the time to failure under constant high-temperature stress. Both fatigue and creeping experiments were applied to two FGM variants, namely SS316L + 20% Inconel 625 + 20% Ti6Al4V and SS316L + 20% Inconel 625 + 20% Inconel 718, and compared against the standard SS316L. These tests provided a complete understanding of the long-term performance of the FGMS and confirmed their better stability and mechanical integrity in the high-stomach, high-illustrated environment [26]

2.4 Advanced Manufacturing Process of Test Coupon

This section highlights the experimental evaluation of the thermal and mechanical behavior of SS316L and the experimental assessment of a newly developed functionally graded material (FGMS) under both high and low temperature conditions. The primary objective is to assess and compare the performance of these materials, particularly two FGMS: SS316L + 20% Inconel 625 + 20% Ti6Al4V and SS316L + 20% Inconel 625 + 20% Inconel 718, when exposed to exit thermal environments compared to traditional SS316L. Test coupons were fabricated using advanced manufacturing techniques, including DED and PM, to ensure the controlled gradient structure and thickness of the layer. These coupons were then subjected to a series of standardised mechanical tests to evaluate tensile strength, hardness, fatigue resistance, and creep behaviour. For low-temperature analysis, samples were cooled to sub-zero conditions (°C and below) to assess their sensitivity, crack initiation, and strength retention. Mechanical properties, such as stiffness and fracture behavior, were recorded to determine their purpose in a cryogenic or cold-vacuum environment. The aerospace and power generation industries conducted high-temperature testing at temperatures of 300 °C, 600 °C, and 1000 °C to simulate the operating stresses in these industries. At these high temperatures, the material was tested for tensile properties, hardness decline, crawling resistance, and thermal stability. The target temperature was to determine the threshold at which FGMS maintain their structural integrity and perform to the standard of SS316L. This practical evaluation simultaneously provides significant insight into the effectiveness of FGM in handling thermal stress and mechanical load. The results will support the verification of these materials for high-protest applications, which require long-term reliability under fluctuating thermal conditions.

2.5 Thermoplastic Materials

In this experiment, three commonly used thermoplastic materials, PETG, PLA, and ABS, with a 1.75 mm filament diameter, were selected to evaluate their tensile strength under standardized conditions. These ingredients were printed

on a tensile coupon using controlled parameters (100% infill density, 0.2 mm layer thickness, 0.5 mm nozzle diameter, and 30 mm/s print speed) to ensure consistency and repeatability. At least four samples were printed for each material to achieve statistically reliable results. The tensile test was conducted using a 10 kN load cell on the Instron 5969 universal testing machine. The tests followed the ASTM D638 standard, with minor amendments to accommodate the geometry and failure characteristics of the 3D printed materials. In particular, the tensile coupon design was modified to reduce the width of the neck and promote controlled necking, thereby increasing the sweep length of the grip plaque and avoiding premature failure outside the gauge length. This modification was supported by previous studies, which aimed to improve data accuracy in printed samples. Each sample was loaded at a continuous rate of 5 mm/min, the lowest rate allowed by ASTM D638 guidelines to ensure uniform stress distribution. The samples were clamped using a flat jaw rated for a maximum load of 50 kN, and additional care was taken to ensure a secure grip and minimize slippage, thereby maintaining sample alignment. Post-testing, the collected data were used to calculate the significant mechanical properties, including the Modulus of Elasticity (E) and the ultimate tensile strength (UTS), which were then statistically processed and compared across three ingredients. This process was required to evaluate the mechanical reliability of these thermoplastics in the additive manufacturing application, where load-bearing performance is important. Figure 2 shows the machine setup for tensile strength.

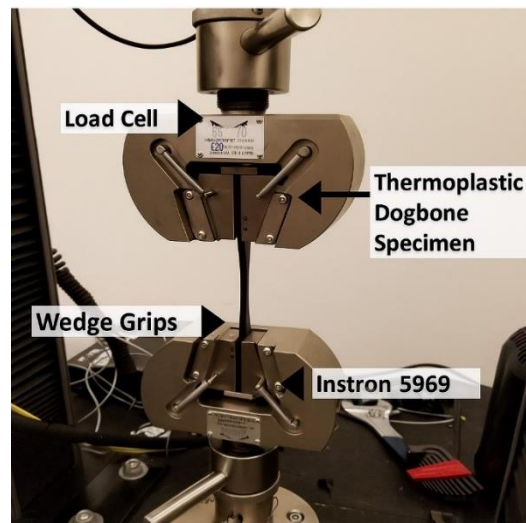


Figure 2. Machine setup for tensile test

The specimens used in the tensile tests were made on a Prusa i3 3D printer. The process settings were set to 100% fill density, a 0.2 mm layer thickness, a 30 mm/s printing speed, and a 0.5 mm nozzle size to avoid fill pattern issues. To prevent most layers from running at an angle along the entire width of the piece, the samples were printed on the print bed at a 45° angle. Research ensured that the start and finish of each layer were outside the coupon's limited area to prevent cracks from occurring when the printer starts or stops between layers. These guidelines remained constant across all samples. An example of a PLA printed tensile test strip is shown in Figure 3.



Figure 3. PLA tensile coupon

Three distinct temperature ranges — 40, 65, and 170 °F — were used to measure the effect of temperature on mechanical properties. The samples were submerged in hot water at 170 °F until they stabilized at that temperature in order to give the 170 °F (hot) working temperature. Using heated pliers, the samples were quickly removed from the hot water and placed into the tensile testing apparatus. To prevent heat transmission, a heat gun was employed to warm the vicinity of the sample and maintain a constant temperature. To lower the temperature of the cold materials to 40 °F, the "cold" operating temperature, they were submerged in an ice bath. The samples were then placed inside the tensile testing device after being removed from the refrigerator using cold pliers. A FLIR thermal image camera was used to verify the temperature throughout each test. Throughout the test, the lab's temperature was maintained at 65 °F; samples were taken at ambient temperature prior to and during the test to verify this.

2.6 Aluminium Alloy

Table 2 highlights the key parameters employed in the laser powder bed fusion (LPBF) process for both the contour and wholesale regions of the build. For both regions, the laser power was maintained at 370 W, and the layer thickness was set to 60 μm to ensure the formation of a uniform melt and a consistent layer. However, the speed of the scan varies greatly, with a slow speed of 300 mm/s to increase the accuracy of the surface along the contour area, while the wholesale area uses a high-speed of 2000 mm/s to optimize build efficiency. Additionally, the hatch distance, which represents the vacancy between the sustainable laser scan lines, was specified as 90 μm for bulk but marked as 1 for the contour, indicating that no hatching was implemented in that area, possibly to avoid overlapping and maintain external edges.

Table 2. Parameter of the LPBF process

Parameter	Contour	Bulk
Laser Power	370	370
Scan Speed	300	2000
Hatch Distance	-1	90
Layer Thickness	60	60

2.7 Manufacturing of Functionally Graded Materials

WAAM is an advanced process invented through the combination of two state-of-the-art technologies: welding and additive manufacturing. WAAM utilizes wire as feedstock and is more efficient and economical due to the use of wire as material feedstock compared to the powder-based methods. This process is a rapid production method for metal parts that utilizes minimal material waste and is particularly suited for the aerospace, automotive, and maritime industries. The ability of WAAM to build large-scale parts with complex geometries and the associated high deposition rate make it incredibly favourable for manufacturing strong, large-scale parts. Additionally, WAAM easily integrates with computer-controlled processes (CAM) for monitoring and adapting parameters (input variables) like those used in conventional machining, thereby achieving greater accuracy and repeatability. Further development of WAAM is enabled by recent advancements in multi-axis robotics and real-time monitoring, which facilitate the fabrication of structurally integral and efficient components. Consequently, WAAM is increasingly seen as a potential solution for the development of durable, custom metal parts in high-demand areas. At high temperatures, the increased thermal energy causes the molecules or atoms within a material to vibrate more intensely, reducing their ability to stay in their original positions. As a result, the material's atomic structure becomes weakened, leading to a loss of strength, and, at extremely high temperatures, the material can melt. This phenomenon explains why materials exhibit a decrease in strength at elevated temperatures. On the contrary, when a substance is cooled, its molecules slow down and move closer together, resulting in a reduction in the material's volume and an increase in its density, which enhances its structural stability and strength at lower temperatures. Figure 4 illustrates the advanced robotic wire arc additive manufacturing process.



Figure 4. Advanced robotic wire arc additive manufacturing

2.8 High and Low Temperature Simulation Analysis

In this study, two new materials: 1) SS316L mixed with 20% Inconel 625 and 20% Titanium Grade 5, and 2) SS316L mixed with 20% Inconel 625 and 20% Inconel 718 are studied. SS316L is a metal that resists rusting easily and is highly resistant to corrosion. It gets even stronger when mixed with Inconel alloys and titanium. Inconel 625 is a strong metal made mostly of nickel. It performs well in hot conditions and resists rust easily. Inconel 718 is another strong metal that can withstand considerable pulling and maintains its integrity well in the face of temperature fluctuations. Titanium Grade 5 is a type of titanium that is very strong and light. It also does not rust easily. These materials are designed to be stronger, especially in extremely hot and cold temperatures. This helps them stay strong and not break down in tough conditions.

Table 3, which contains the outcome of temperature tests on three various materials at two temperature parameters, namely -20°C and $+60^{\circ}\text{C}$. The materials used for the experiment are 100% SS316L and two types of FGMs that are created from a combination of SS316L and other alloys. In the table below, information is presented on the UTS and the Yield strength (0.2% proof) of each material at the given temperatures. The results provide information about the characteristics of these materials under different thermal gradients.

Table 3. Temperature test

S. No.	Parameter	Unit	100% SS316L (-20°C / $+60^{\circ}\text{C}$)	FGM - 60% SS316L + 20% Inconel 625 + 20% Ti6Al4V (-20°C / $+60^{\circ}\text{C}$)	FGM - 60% SS316L + 20% Inconel 625 + 20% Inconel 718 (-20°C / $+60^{\circ}\text{C}$)
1	Ultimate Tensile Strength	MPa	550 / 460	732 / 592	1186 / 992
2	Yield Strength (0.2% Proof)	MPa	304 / 186	384 / 302	734 / 602

The three materials analyzed in this study offer distinct compositions, each with unique properties that influence their mechanical performance, especially under varying temperature conditions:

1. Entirely made of SS316L (Stainless Steel 316L), which is one of the most preferred alloys for forming components on account of its high degree of corrosion resistance and acceptable strength characteristics. Austenitic stainless steel, for instance, is composed of iron, chromium, and nickel, and it is used in harsh environments, such as those in chemistry or saltwater, as the metal does not corrode. This further makes it ideal for use in structures, but it possesses a weakness in high temperatures.
2. A combined composition of 60% SS316L, 20% Inconel 625, and 20% Ti6Al4V is known as FGM, a functionally graded material that exhibits the excellent features of all its constituent materials. The addition of a solid-solution strengthener, consisting of INCONEL 625, a high-integrity nickel-based superalloy with remarkable attributes including high strength at elevated temperatures, resistance to heat, oxidation, and corrosion, enhances the material's ability to withstand stress. The incorporation of Ti6Al4V, also known as the Titanium Grade 5 material, increases the material's properties by increasing the strength-to-weight ratio and fatigue characteristics. This combination of alloys provides the material with high strength and relatively low density, making it suitable for use in applications such as aerospace and high-performance engineering.
3. Another FGM is FGM – 60% SS316L + 20% Inconel 625 + 20% Inconel 718, which provides better thermal and mechanical stability compared to the previously discussed composition, due to the inclusion of Inconel 718. Inconel 718 is also a nickel-based superalloy, but it provides markedly greater high-temperature strength and creep resistance, making this material suitable for use in arrangements exposed to intense heat, such as turbine blades or high-performance engines. In this amalgamation, the corrosion resistance property of SS316L, along with the thermal stability of Inconel 625 and Inconel 718, is utilized to develop a material that can resist both high heat and mechanical forces without considerable damage. The combination of SS316L & Inconel 718 means that this FGM retains its good tensile & yield strength at elevated temperatures, superior to both base metals & the other FGM containing Ti6Al4V. This means that the material can be used in applications where high temperature is required and structural stability is paramount.

The following materials explain how the use of alloy gradation enables the control of material characteristics to accommodate specific properties suitable for a particular application complexity in industries, especially those requiring both heat and mechanical properties. When the temperature is increased to $+60^{\circ}\text{C}$, a reduction in UTS and 0.2% YS is observed for all materials, as heat has an adverse effect on the crystal structure and mechanical properties of the alloy. As for 100% SS316L, the UTS decreases to 460 MPa, which can explain the material's sensitivity to heat. Tailored properties, making them suitable for specialized applications across industries that demand both thermal resilience and mechanical strength. For 100% SS316L, the UTS drops significantly to 460 MPa, highlighting the material's susceptibility to heat. The loss of strength is attributed to the increased molecular activity at higher temperatures, which weakens the material's ability to resist deformation under stress. In the case of FGM (SS316L + Inconel 625 + Ti6Al4V), while the UTS decreases to 592 MPa, this composite material retains greater tensile strength compared to pure SS316L. Alloying of Inconel 625 and Ti6Al4V increases the capacity of this particular alloy under thermal stress and, in turn, improves the engineering properties. These materials can resist high-temperature corrosion or maintain their overall structure, albeit with some loss of strength, in response to such an attack. Pseudoplastic FGM features the FGM (SS316L + Inconel 625 + Inconel 718) with the reported highest UTS of 992 MPa, making it suitable for specialized applications across industries that demand both thermal resilience and mechanical strength. This makes the material ideal for use in applications where there will be constant exposure to heat, as it loses far less strength than the other two materials.

In terms of yield strength (0.2% Proof), the decline in performance follows a similar pattern. The characteristic of 100% SS316L decreases significantly as its yield strength decreases to 186 MPa, indicating that the material unexpectedly loses a substantial portion of its capacity to withstand plastic deformation under stress at higher temperatures. FGM (SS316L + Inconel 625 + Ti6Al4V) shows a comparatively better yield strength of 302 MPa, which underscores the advantage of integrating Inconel 625 and Ti6Al4V. These elements contribute to the alloy's improved strength retention

under thermal conditions, making it more resistant to deformation than pure SS316L. FGM (SS316L + Inconel 625 + Inconel 718) stands out with a yield strength of 602 MPa, the highest in this comparison. Inconel 718 is an enhanced superalloy that retains its mechanical strength and does not undergo deformation at elevated temperatures. This makes it well-suited for high-temperature operating environments where part failure cannot be tolerated, such as aerospace and high-end industrial usage. Raising the temperature to +60°C results in uniform deterioration of strength and yield strength for all materials. Once again, the FGM with Inconel 718 demonstrates the highest values of strength and thermal stability among all four tested materials.

When subjected to high temperatures, for example, +60°C, several changes occur at the molecular level within the material. The atoms or molecules acquire more kinetic energy, and as a result, they move more and vibrate in positions of fixed lattices. This leads to reduced mechanical strength and other related effects, such as softening or even melting, depending on the type of material and the level of heat exposure. This behavior is evident in the decrease in UTS and yield strength for all the tested materials. Since temperature affects the material's resistance to deformation under stress, as the temperature increases, the resistance decreases. However, the incorporation of Inconel 718 into the FGM compositions has a significant influence on heat due to Inconel 718's ability to maintain mechanical properties at high temperatures. This results in FGM with Inconel 718 having a higher rate of resistance to high-temperature degradation compared to the others, as indicated by the UTS and yield strength at +60 °C. Figure 5 shows the computerized temperature testing chamber.

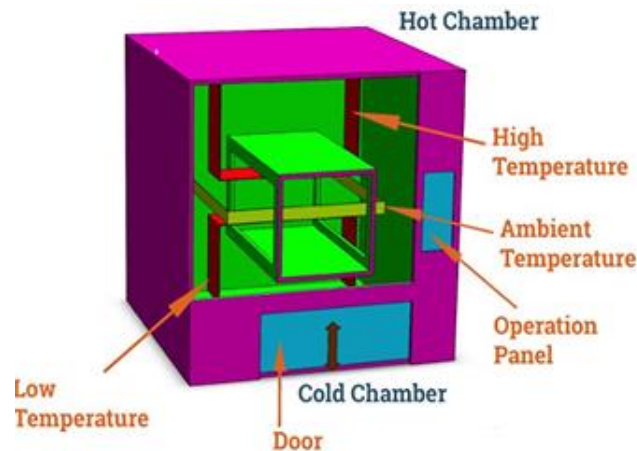


Figure 5. Computerized temperature testing chamber

On the other hand, at relatively low temperatures, such as -20°C, the material's characteristics undergo drastic changes. Cooling causes the velocity with which molecules or atoms are moving to decrease, and hence they come closer together, resulting in a denser packing. This means that due to the tighter arrangement, there is an improvement in the tensile and yield strength of the material, resulting from an increased ability to withstand external forces. At such lower temperatures, all the materials investigated exhibit higher strength, as they are less easily deformed. In particular, the use of Inconel alloys (Inconel 625, Inconel 718) in FGMs enhances performance in cold environments. These alloys, which enhance thermal and mechanical properties, add strength and durability to the FGMs, allowing them to withstand stress and deformation better than SS316L. These characteristics of molecular stability, along with the inherent properties of Inconel alloys, make FGMs, including Inconel 718, much more reliable at both low and high temperatures than the SS316L material used alone.

At high temperatures, the thermal energy within the material increases significantly. It causes the molecules or atoms of the material to vibrate more violently. Figure 6 (a), (b), and (c) illustrate the high- and low-temperature tests conducted on the FGM materials, where the high-mobility action weakens the bonds between molecules or atoms. The bond that holds the structure of a material together. When the temperature increases, these bonds become less stable and their ability to resist external forces decreases. This is because materials soften or melt at high temperatures. This results in a significant reduction in mechanical strength. For example, in metals, this can reduce tensile strength, yield strength, and hardness. Basically, Atoms or molecules cannot maintain a fixed position in the lattice structure of the material. This leads to structural breakdown and the onset of melting. At the same time, the opposite effect is achieved when the material is cooled. A drop in temperature causes the molecule or atom to lose kinetic energy and move more slowly. As a result, the force between them is strong. This causes the particles to move closer together, thereby reducing the material's volume. This shrinkage increases the material's density. This is because there are more particles contained in a smaller space. Materials in this state generally have greater strength and rigidity because their molecular or atomic structure is more tightly bound together. Increased density and lower temperature make the material more resistant to deformation and mechanical stress. Therefore, it has better strength in colder environments.

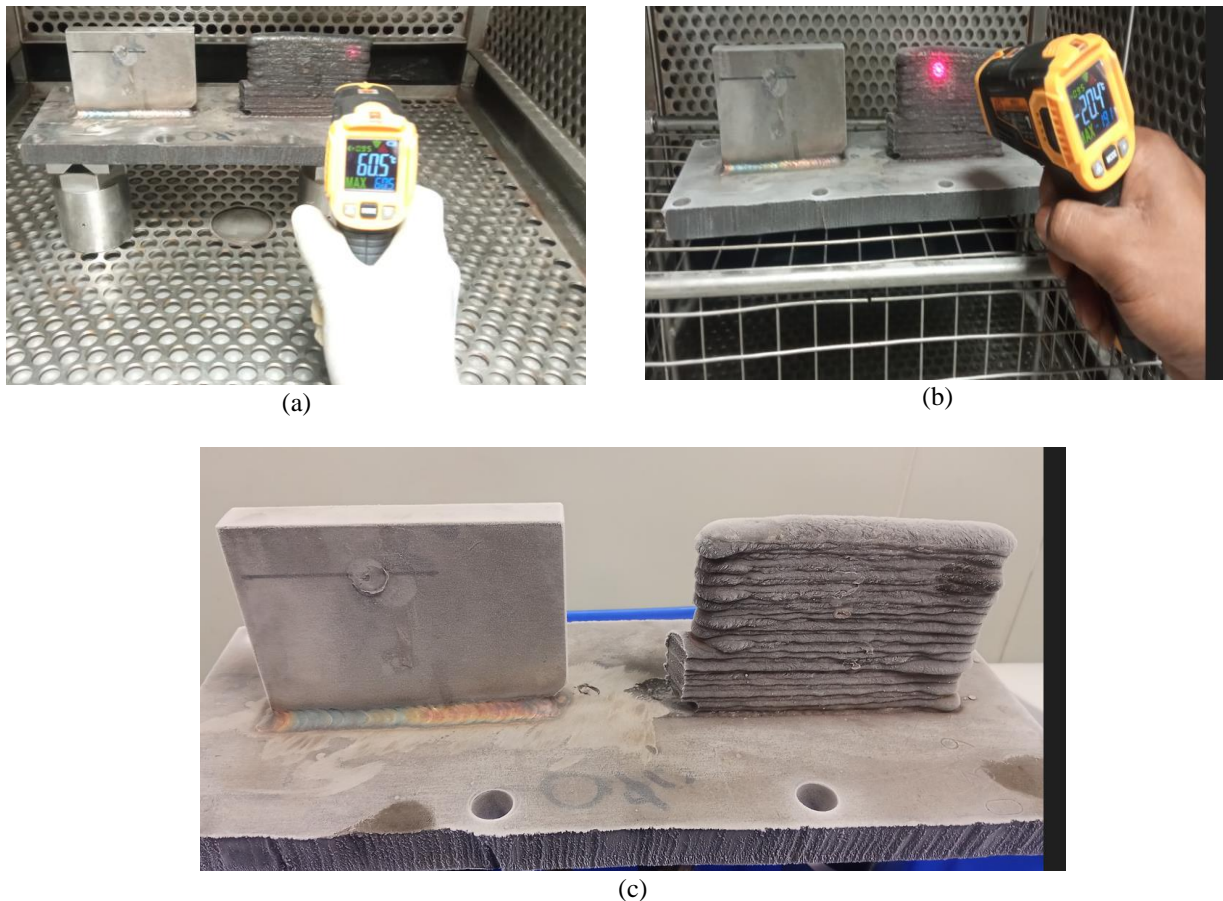


Figure 6. FGM Specimen set on computerized temperature testing chamber: (a) 100% SS316L, (b) FGM - 60% SS316L+20% INCONEL 625+20% Ti6Al4V, and (c) FGM - 60% SS316L+20% INCONEL 625+20% Inconel 718

2.9 15-5 PH Stainless Steel

To avoid oxidation, the AM samples were created in an argon atmosphere using an EOSINT M270 machine equipped with a 200 W Yb fiber laser (wavelength 1070 nm). A 170-watt laser, a scanning speed of 1250 mm per second, a spot size of 50 μm , a hatch spacing of 100 μm , and a layer thickness of 30 μm were the parameters that were employed. The powder called EOS Stainless Steel PH1 was used. It mainly contains the following elements: Cu (25–45%), Ni (35–55%), Cr (14–15%), and the remainder is Fe. The round rods, which are 15 mm wide and 90 mm long, were then heated at a low temperature to reduce stress. Additionally, TM 15-5 PH SS round bars, 25 mm wide, were purchased. The densities of both materials were determined to be approximately 7.8 g/cm^3 after applying Archimedes' principle to the density data. The Instron 5982 testing equipment and a creep tester were used to manufacture these rods into tensile and creep samples, which were subsequently tested at 593°C at a strain rate of 10^{-3} s^{-1} . After sectioning, mounting, grinding, and polishing the specimens before etching them with Aqua Regia, one AM sample was subjected to tensile testing at room temperature. Furthermore, samples of microhardness were produced. The tribological properties of AA7168 are also similarly utilized in aerospace structures, and tribological characterization of the Scalmalloy parts was performed, including Vickers microhardness tests on each sample face with 17 indentations. After being jet-coated and examined using Transmission Electron Microscopy (TEM), thinner metal parts were examined using SEM, which operates at 10 kV to examine the areas of fracture. To ensure interfaces are free of damage for Electron Back Scatter Diffraction (EBSD) investigation, specimens were prepared exactly as in the TEM method.

3. RESULTS AND DISCUSSION

3.1 Microhardness Testing

The longitudinal and transverse cross-sections of the TM and AM samples were subjected to Vickers microhardness examination. Table 1 summarizes the mechanical properties of the tested materials at -20. Compared to the AM material, the TM material is softer. The hardness values also demonstrate that the AM material is significantly more rigid than the TM material. Notably, FGM composed of SS316L + Inconel 625 + Inconel 718 demonstrated the highest mechanical resistance, recording a UTS of 992 MPa and a yield strength of 602 MPa at +60°C, compared to SS316L's values of 460 MPa and 186 MPa, respectively. Fatigue testing was conducted under controlled cyclic loading to determine the number of cycles to failure for each material configuration. Results showed improved fatigue life in FGMs, attributed to the enhanced microstructural stability and superior resistance to crack initiation provided by Inconel and Ti6Al4V phases. Among the tested samples, FGM (SS316L + Inconel 625 + Inconel 718) exhibited the most extended fatigue life due to

the synergistic reinforcement of two high-performance nickel-based alloys. Creep testing was conducted at high temperatures and under constant loads to evaluate long-term material deformation. The Inconel-rich FGM showed the lowest creep rate, validating its suitability for applications requiring long-duration exposure to heat and stress. Table 1 summarizes the observed mechanical performance of all three materials at -20°C and $+60^{\circ}\text{C}$.

Table 1. Summary of mechanical properties of tested materials at -20°C and $+60^{\circ}\text{C}$

Material Configuration	Temperature ($^{\circ}\text{C}$)	UTS (MPa)	Yield Strength (MPa)	Fatigue Resistance (Qualitative)	Creep Behavior (Qualitative)
100% SS316L	-20	550	304	Moderate	Moderate
	$+60$	460	186	Low	High Creep Rate (Poor Creep Resistance)
FGM: SS316L + Inconel 625 + Ti6Al4V	-20	732	384	High	Improved Creep Resistance
	$+60$	592	302	Moderate	Better Than SS316L
FGM: SS316L + Inconel 625 + Inconel 718	-20	1186	734	Very High	Excellent (Lowest Creep Rate)
	$+60$	992	602	High	Very Low Creep Rate (Highly Stable)

3.2 Tensile Properties

Uniaxial tensile testing was performed on the TM and AM composites at 593°C with a strain rate of 10^{-3}s^{-1} . The theoretical stress-engineering strain curves for the TM and AM materials are displayed in Figure 7. It is found that the TM and AM materials have comparable yield strengths and ultimate bending strengths, suggesting that they have a minimal possibility for strain stiffening. The AM composite shows a nearly 30% greater yield strength and a 32% higher ultimate tensile strength compared to the TM material.

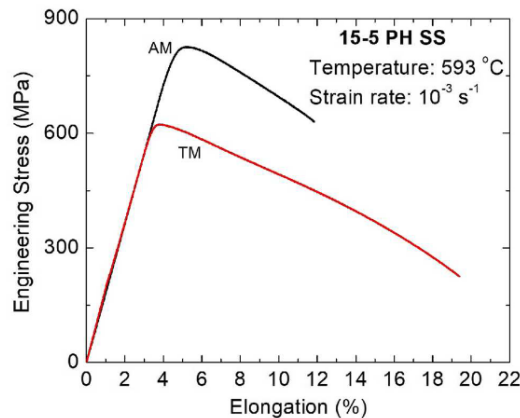


Figure 7. Engineering stress-strain curve for 15-5 PH SS traditionally manufactured and additively manufactured 15-5 PH SS

3.3 Creep Properties

The TM and AM specimens in this investigation underwent creep rupture tests with an applied stress of 211 MPa and an ambient temperature of 593°C . The matching creep curves for the TM and AM materials are displayed in Figure 8. These creep tests are best described as stress rupture tests due to their brief duration. The high temperature and stress levels employed in the creep tests are the reason why the creep curves lack clear primary and steady-state phases. It was discovered that the AM material had a rupture life of 157.2 hours, as opposed to 121.2 hours for the TM material. The minimal creep rate for the AM material is therefore 0.0003%/h, whereas for the TM material it is 0.038%/h. It was discovered that the lowest creep rate in a 15-5 PH SS that had been wrought and annealed was 0.015%/h [13]. The findings of the creep test clearly demonstrate that the AM material exhibits superior creep properties compared to the TM material. To fully comprehend the distinctive creep behavior of the AM materials, further creep studies are necessary.

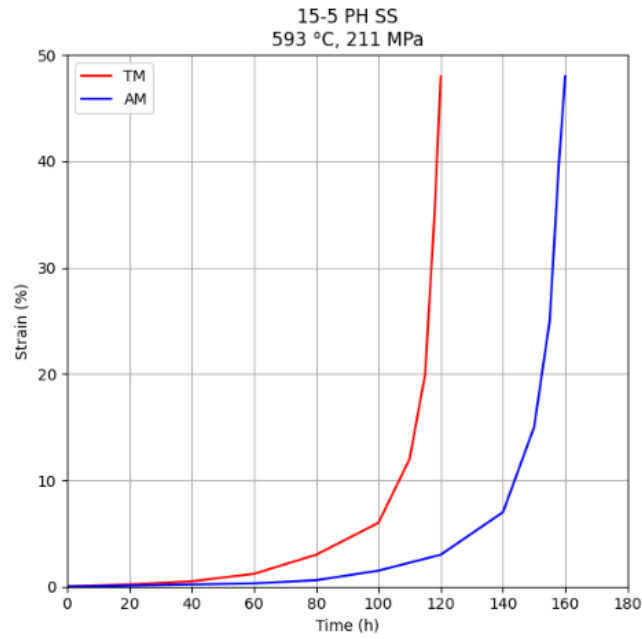


Figure 8. TM and AM creep curves

Figure 9 provides a few examples of engineering stress-strain curves, including curves obtained at (a) room temperature (RT), (b) 125 °C, (c) 250 °C, and (d) 450 °C. Each graphic shows a typical curve for each of the compared construction directions. A sample machined from a cylindrical specimen at a polar angle of 0° is the subject of the data shown in Figure 7(a), utilizing identical conditions as the other samples. For each graph, the same x- and y-axis scaling has been used to highlight the variations in strength and ductility.

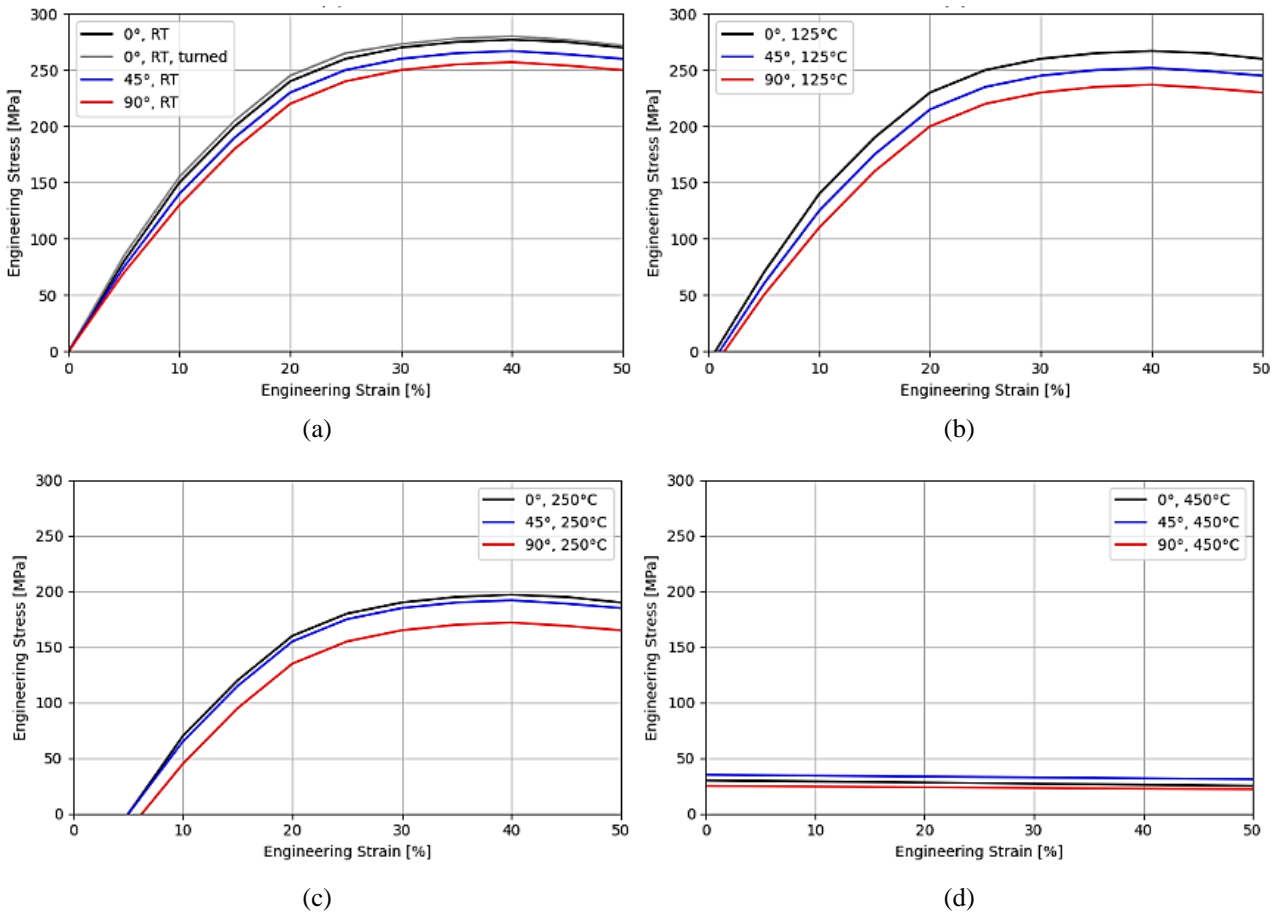


Figure 6. Engineering stress versus strain curves for different build orientations and test temperatures: (a) room temperature, (b) 125 °C, (c) 250 °C, and (d) 450 °C

3.5 W-CU Functionally Graded Materials

The first components were commercially available powders of W, Ni, Mn, and Cu, with a purity level exceeding 99.9%. The greatest particle sizes for “Ni, Cu, and Mn were 10, 30, and 63 μm ”, respectively, whereas the lowest range for W was 7.5–8.5 μm . Table 4 displays the findings of the first X-ray fluorescence (XRF) study of powder performed with an X’Unique II Ge111 spectrophotometer (detection limit $\frac{1}{4}$ 1 ppm). A high-energy ball mill (SPEX 8000 Mixer/Mill) was used to mechanically alloy the Ni, Cu, and Mn metallic powders to produce a binder alloy (BA).

Table 4. Chemical composition of the initial powder according to XRF

Cu Powder		W Powder		Mn Powder		Ni Powder	
Element	wt.%	Element	wt%	Element	wt%	Element	wt.%
Cu	99.96	W	99.92	Mn	99.96	Ni	99.97
Pb	0.030	S	0.06	S	0.024	Fe	0.012
Fe	0.006	Fe	0.02	Ni	0.016	Mn	0.011
Ca	0.004	-	-	-	-	S	0.007

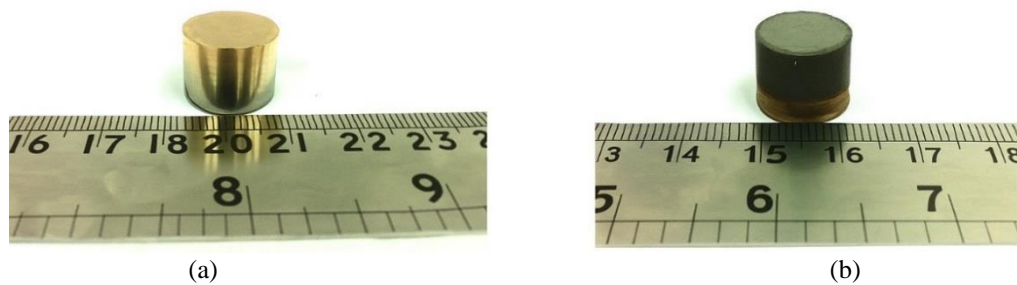


Figure 7. (a) Green body of the W–Cu FGM (Cu on the top side and W on the bottom side) and (b) A sintered compact of the W–Cu FGM (W on the top side and Cu on the bottom side)

It is essential to note that each of the 10 composite powders had a 9:1 weight ratio of W to BA. Additionally, the settings were a ball-to-powder weight ratio of 1:1, a rotation velocity of 250 rpm, and a mixing time of 45 minutes. Together with the layer of Cu powder, the other composite powder layers were carefully inserted into the steel die. A light pressure of up to 1000 MPa was applied after each layer was applied. The green specimen was then removed from the die. The green W–Cu FGM sample is displayed in Fig. 9a. The solid-state sintering process was carried out for three hours at 1000 °C under vacuum and at a rate of 10 °C/min to produce the green compact.

The primary objective of this study is to understand how temperature changes impact the mechanical integrity and structural performance of materials, specifically by comparing two recently developed FGMs with conventional 100% SS316L stainless steel. The investigation examined their UTS and yield strength (0.2% proof stress) at extreme temperature points: -20°C and $+60^{\circ}\text{C}$. The results clearly establish that both FGMs significantly outperform SS316L across these thermal conditions, especially the FGM composed of SS316L, Inconel 625, and Inconel 718, which exhibited the highest values for both UTS and yield strength. At low temperatures (-20°C), all materials showed an increase in mechanical strength. This phenomenon aligns with physical theory: lower temperatures reduce atomic vibrations and increase atomic packing density, thereby enhancing resistance to deformation. However, FGMs demonstrated superior performance compared to SS316L due to their tailored compositional gradients. Inconel 718, renowned for its high-temperature structural stability and excellent low-temperature toughness, significantly contributes to the improved behavior of the FGM under sub-zero conditions. Current high-performance alloys incorporated within the SS316L matrix are designed to increase tensile strength and yield stress while enhancing ductility, making their incorporation suitable for FGM use in cryogenic or aerospace applications. These applications require the material to function in extreme cold and withstand significant recoil without failure. On the other hand, when tested at elevated temperatures ($+60^{\circ}\text{C}$), all materials tested experienced a decrease in both yield and UTS. The reduction observed is a result of increased atomic kinetic energy, which weakens the material’s structural integrity and load-bearing capacity by breaking interatomic bonds.

Finally, the FGMs exhibited lower and slower decreasing strength than SS316L, with the Inconel 718-based FGM having the highest thermal resilience. Creep and oxidation resistance can be highly critically evaluated through this behavior lens, since Inconel-based alloys exhibit stronger behavior in these properties. Nickel-based superalloys, such as Inconel 625 and 718, retain their microstructural stability and mechanical strength despite operating in a hot environment, thanks to gamma prime, γ' precipitate hardening mechanisms and stable phase structures. Unlike SS316L, these materials resist grain boundary sliding and dislocation movement (common modes of high temperature deformation) through stable interfaces that do not soften due to phase instability and diffusion-related degradation. The performance of FGMs was superior to that of SS316L. The effect of thermal degradation was demonstrated by UTS (992 MPa at $+60^{\circ}\text{C}$ vs. 460 MPa for SS316L), while retaining up to 60% of the creep resistance of SS316L for regions requiring higher creep resistance. This is the result of Inconel 718’s outstanding grain boundary stability, which limits creep and fatigue at high temperature.

Similarly, with the gradient architecture in FGMs, the stresses are better distributed, resulting in a reduction in residual stresses at dissimilar material interfaces. Minimizing the amount of stress concentration zones, which typically occur in solid materials and can act as crack or failure initiators, is a design advantage of the proposed technique. Synergistic strengthening then results in a single structure, as would otherwise be impossible, that could slowly transition from a ductile base (SS316L) to stronger and more heat-resistant alloys (Inconel 625 and 718 or Ti6Al4V). Consequently, strength, ductility, and thermal stability are simultaneously improved under both low and high temperatures compared to SS316L, which utilizes FGMs that rely on their engineered composition and microstructural design. In brief, FGMs achieve more than just better performance; they enable material efficiency through design customization—materials can be chosen to be spatially variable, allowing them to meet specific operational needs. The key result is that the control by FGMs over SS316L is not due to fortuitous material substitution, but rather to the incorporation of performance-enhancing phases and gradient design. These FGMs are now considered highly adaptable and reliable materials for next-generation applications in aerospace, power generation, nuclear systems, and industries where extreme operating conditions are the norm. These results support future material development strategies that utilize functionally graded, tailored systems, as opposed to traditional homogeneous alloys.

4. CONCLUSIONS

This research successfully demonstrated its stated objectives, as well as the feasibility, performance, and potential of novel multi-phase FGMs under extreme thermal conditions. Two advanced manufacturing processes were used to successfully fabricate two different configurations of FGM consisting of 60% SS316L, 20% Inconel 625 alloy (in weight %), and either 20% Ti6Al4V or Inconel 718. The first control was achieved through the precise control of gradient composition and layer thickness, resulting in a smooth transition of material properties throughout the samples. Secondly, tensile strength, yield strength, fatigue resistance, and creep behavior experiments of S355F structure steel were conducted at both -20°C and $+60^{\circ}\text{C}$, in relation to the second objective. The results showed definitively that both FGMs outperformed the conventional SS316L (at elevated t , the FGM containing Inconel 718 had a UTS of 992 MPa and yield strength of 602 MPa compared to 460 MPa and 186 MPa of SS316L, respectively). In all cases, at lower temperatures, performance improved as density increased. FGMs, however, continued to provide a better overall performance due to their engineered composition. Finally, the influence of such a gradient composition on thermal and mechanical performance has been investigated. The results confirmed that the smooth transition in material phases enhanced stress distribution and microstructural stability, enabling the FGMs to resist deformation and maintain integrity under cyclic thermal and mechanical loads. This study, therefore, not only validates the design and manufacturing approach for FGMs but also reinforces their applicability in demanding industrial sectors such as aerospace, power generation, and chemical processing. Future research should extend this work by incorporating long-term environmental exposure, multi-axial loading conditions, and detailed microstructural evolution analysis to refine further the applicability and reliability of FGMs in real-world high-performance environments.

ACKNOWLEDGEMENTS

The authors sincerely acknowledge the support from the Karpagam Academy of Higher Education, Coimbatore, for their valuable insights and support throughout the study. This study was not supported by any grants from funding bodies in the public, private, or not-for-profit sectors.

CONFLICT OF INTEREST

The authors declare no conflicts of interest to report regarding the present study.

AUTHORS CONTRIBUTION

K. Sainath (Conceptualization; Methodology; Investigation; Data curation; Formal analysis; Validation; Writing -original draft; Visualisation, Writing - Editing)

R. Karuppasamy (Supervision; Writing - review)

S. Prabakaran (Supervision; Writing – review)

AVAILABILITY OF DATA AND MATERIALS

The data supporting this study's findings are available on request from the corresponding author.

ETHICS STATEMENT

Not applicable

REFERENCES

- [1] M. Margini, D. Karpov, Y. Swolfs, C. Breite, Y. Lee, M. Mavrogordato, et al., “Hard X-ray nanoscale imaging of carbon fibre composites using near-field ptychography,” *e-Journal of Nondestructive Testing*, vol. 29, no. 3, pp. 1-6, 2024.
- [2] A. Lahbazi, I. Goda, J.-F. Ganghoffer, “Size-independent strain gradient effective models based on homogenization methods: applications to 3D composite materials, pantograph and thin-walled lattices,” *International Journal of Composite Structures*, vol. 284, pp. 115065–115075, 2022.
- [3] B. Wang, S. Zhong, T.-L. Lee, K. S. Fancey, J. Mi, “Nondestructive testing and evaluation of composite materials/structures: a state-of-the-art review,” *Advances in Mechanical Engineering*, vol. 12, no. 4, pp. 1–28, 2020.
- [4] R. Gupta, D. Mitchell, J. Blanche, S. Harper, W. Tang, K. Pancholi, et al., “A review of sensing technologies for nondestructive evaluation of structural composite materials,” *Journal of Composites Science*, vol. 5, no. 12, pp. 319–339, 2021.
- [5] N. M. Ngoc, V.-N. Hoang, D. Lee, “Concurrent topology optimization of coated structure for non-homogeneous materials under buckling criteria,” *Engineering with Computers*, vol. 38, no. 6, pp. 5635–5656, 2022.
- [6] S. Nikbakht, S. Kamarian, M. Shakeri, “A review on optimization of composite structures part II: Functionally graded materials,” *Composite Structures*, vol. 214, pp. 83–102, 2019.
- [7] A. A. Daikh, M. S. A. Houari, M. O. Belarbi, S. Chakraverty, M. A. Eltaher, “Analysis of axially temperature-dependent functionally graded carbon nanotube reinforced composite plates,” *Engineering with Computers*, vol. 38, suppl. 3, pp. 2533–2554, 2022.
- [8] P. Nayak, A. Armani, “Optimal design of functionally graded parts,” *Metals*, vol. 12, no. 8, pp. 1335–1348, 2022.
- [9] L. K. Sharma, G. Bhardwaj, N. Grover, “Finite element framework for static analysis of temperature-dependent IHSdT-based functionally graded CNT reinforced plates,” *Mechanics Based Design of Structures and Machines*, vol. 51, no. 9, pp. 5318–5339, 2023.
- [10] J. Patil, C. Jadhav, N. Chandel, V. Varghese, “Memory-dependent response of the thermoelastic two-dimensional functionally graded rectangular plate,” *Mechanics of Time-Dependent Materials*, vol. 28, no. 2, pp. 123–144, 2024.
- [11] N. Sargent, “Integrated computational and experimental design of functionally graded materials made with additive manufacturing,” *PhD Thesis*, University of Pittsburgh, 2024.
- [12] R. Chiba, Y. Sugano, “Optimisation of material composition in functionally graded plates for thermal stress relaxation using statistical design support system,” *Curved and Layered Structures*, vol. 11, no. 1, p. 20220221, 2024.
- [13] M. D. Allen, “Systematic design of metallic functionally graded materials & structures,” *PhD Thesis*, University of Cambridge, 2025.
- [14] G. Maciejewski, Z. Mróz, “Optimization of functionally gradient materials in valve design under cyclic thermal and mechanical loading,” *Computer Assisted Methods in Engineering and Science*, vol. 20, no. 2, pp. 99–112, 2013.
- [15] D. Punera, T. Kant, “A critical review of stress and vibration analyses of functionally graded shell structures,” *Composite Structures*, vol. 210, pp. 787–809, 2019.
- [16] F. Althoey, E. Ali, “A simplified stress analysis of functionally graded beams and influence of material function on deflection,” *Applied Sciences*, vol. 11, no. 24, pp. 11747–11760, 2021.
- [17] C. J. Ejeh, I. Barsoum, R. K. A. Al-Rub, “Flexural properties of functionally graded additively manufactured AlSi10Mg TPMS latticed-beams,” *International Journal of Mechanical Sciences*, vol. 223, p. 107293, 2022.
- [18] B. Bocklund, “Computational design of additively manufactured functionally graded materials by thermodynamic modeling with uncertainty quantification,” *PhD Thesis*, The Pennsylvania State University, 2021.
- [19] S. Rahman, “A novel approach to optimize material distributions of rotating functionally graded circular disk under minimum and prescribed stresses,” *Materials Today Communications*, vol. 106, pp. 106620–106629, 2023.
- [20] M. E. Stender, L. L. Beghini, J. D. Sugar, M. G. Veilleux, S. R. Subia, T. R. Smith, et al., “A thermal-mechanical finite element workflow for directed energy deposition additive manufacturing process modeling,” *Additive Manufacturing*, vol. 21, pp. 556–566, 2018.
- [21] A. Kiran, J. Hodek, J. Vavrik, M. Urbánek, J. Dugan, “Numerical simulation development and computational optimization for directed energy deposition additive manufacturing process,” *Materials*, vol. 13, no. 11, pp. 2666–2678, 2020.
- [22] A. Pasha, B. Rajaprakash, “Fabrication and mechanical properties of functionally graded materials: A review,” in *Materials Today: Proceedings*, vol. 52, pp. 379–387, 2022.

- [23] Y. Li, Z. Feng, L. Hao, L. Huang, C. Xin, Y. Wang, et al., “A review on functionally graded materials and structures via additive manufacturing: from multi-scale design to versatile functional properties,” *Advanced Materials Technologies*, vol. 5, no. 6, p. 1900981, 2020.
- [24] A. Mehditabar, G. H. Rahimi, S. E. Vahdat, “Mechanical properties of Al 25 wt.% Cu functionally graded material,” *Science and Engineering of Composite Materials*, vol. 26, no. 1, pp. 327–337, 2019.
- [25] M. D. Demirbas, “Thermal stress analysis of functionally graded plates with temperature-dependent material properties using theory of elasticity,” *Composites Part B: Engineering*, vol. 131, pp. 100–124, 2017.
- [26] V. A. Popovich, E. V. Borisov, V. Heurtebise, T. Riemslog, A. A. Popovich, V. S. Sufiiarov, “Creep and thermomechanical fatigue of functionally graded Inconel 718 produced by additive manufacturing,” in *TMS 2018 — 147th Annual Meeting & Exhibition Supplemental Proceedings*, pp. 85–97, 2018.